Gaussian Curvature Criterion based Random Sample Matching for Improved 3D Registration

Faisal Azhar, Stephen Pollard and Guy Adams
HP Labs, Bristol, U.K.

Keywords: Gaussian Curvature, 3D Registration, Matching, Point Cloud, Hash Table.

Abstract: We propose a novel Gaussian Curvature (GC) based criterion to discard false point correspondences within the RANdom SAmple Matching (RANSAM) framework to improve the 3D registration. The RANSAM method is used to find a point pair correspondence match between two surfaces and GC is used to verify whether this point pair is a correct (similar curvatures) or false (dissimilar curvatures) match. The point pairs which pass the curvature test are used to compute a transformation which aligns the two overlapping surfaces. The results on shape alignment benchmarks show improved accuracy of the GRANSAM versus RANSAM and six other registration methods while maintaining efficiency.

1 INTRODUCTION

Three-dimensional (3D) point cloud registration is used to align CAD or full 3D scans with partial scan to perform robotic bin picking, 2D and 3D inspection or authentication, and full 3D scene reconstruction. Partial views, clutter, illumination variation and noise in scan from the 3D sensor present a significant challenge to any 3D registration approach. Hence, Random Sample Consensus (RANSAC) (Fischler and Bolles, 1981) model fitting scheme, which finds a small number of correct point correspondences to align the scene to the model, is often used as a standard approach to deal with such challenges. In addition, extra geometric features or descriptors (invariant under rigid transformation) are used in the RANSAC scheme to prune out mismatched points in a matching and registration scenario. Such geometric features often require computationally expensive accumulation or differientiation of local information, e.g., volumetric invariant (Gelfand et al., 2005), mean curvature, Gaussian curvature (GC), etc (Besl and Jain, 1986). Hence, we are motivated to propose a simple and easy implementation of a Gaussian curvature check in RANSAM (Winkelbach et al., 2006) framework to prune mismatched points in order to improve accuracy and maintain efficiency of 3D registration. We show that an efficiently computed GC descriptor used for pruning can bring improvement to the exisiting RANSAM approach. However, comparison of different geometric descriptors is not within the scope of this paper.

The key observation is that Gaussian curvature provides a simple but powerful descriptor, so that points with different curvatures are unlikely to contribute to a correct correspondence, and thus can be discarded. We evaluate this idea on a number of shape alignment benchmarks and show improvement over several of them. The main contribution of our work is the inclusion of the discrete Gaussian curvature check into the RANSAM framework for discarding unlikely feature point correspondences during the shape alignment. The advantages of our approach are: (a) improvement in accuracy, (b) minimal computational cost and (c) simple and easy integration into existing registration approaches.

This paper is organised as follows. Section 2 presents literature review. Section 3 presents our GRANSAM method. Section 4 compares the performance of the GRANSAM with RANSAM and six other global registration methods. Section 5 concludes the paper.

2 RELATED WORK

Most popular 3D feature descriptors include point feature histogram (PFH) (Rusu et al., 2008), fast point feature histogram (FPFH) (Rusu et al., 2009), signature of histogram of orientations (SHOT) (Tombari et al., 2010), etc. RANSAC is used to repeatedly es-

Azhar, F., Pollard, S. and Adams, G.
Gaussian Curvature Criterion based Random Sample Matching for Improved 3D Registration.
DOI: 10.5220/0007343403190325
In *Proceedings of the 14th International Joint Conference on Computer Vision, Imaging and Computer Graphics Theory and Applications (VISIGRAPP 2019)*, pages 319-325
ISBN: 978-989-758-354-4

timate an alignment for a randomly chosen subset of correspondences which is validated on the entire or subset point cloud. PCL (Holz et al., 2015; Rusu et al., 2009) is the sample consensus initial alignment algorithm, from the Point Cloud Library, which uses histogram of point pair features, i.e., FPFH, to obtain a global registration. CZK (Choi et al., 2015) is a method which combines geometric registration of scene fragments with robust global optimization based on line processes for 3D scene reconstruction. Noisy data and partially overlapping point clouds create a significant problem to these methods because they require many repetitions to find a good point correspondence set. In contrast, the FGR (Zhou et al., 2016) method uses a fixed subset of corresponding points, some correct and some not, which are considered together. It aims to iterate towards a solution that selects the correct point matches while discarding the noise using a German McClure objective function within a graduated non-convexity framework. The MFR method in (Faisal Azhar and Adams, 2019) builds upon FGR method but uses weighted median in a re-weighted least squares approach with graduated M-Estimation to rapidly converge to optimal registration. These methods may totally fail to align engineering parts (with significant planar surfaces) because of lack of unique local features and do not always perform well with different views of more general (non-planar surfaces) parts because the descriptor based matching does not always find good point correspondence match suitable for 3D registration. Recently, (Rantoson et al., 2016) introduced registration which uses Gaussian curvature constraint on the randomly sampled point pair matches to improve registration. This method uses DARCES algorithm, which is a computationally expensive procedure, to randomly compare three scene points to all the points in the model to find point matches. Also, redundant comparisons might produce many bad matches in the initial step which can not be resolved using Gaussian curvature constraint in a later step. Also, it uses computationally expensive Eigen value decomposition to compute the Gaussian curvature.

Super4PCS (Mellado et al., 2014) is an optimal linear time output-sensitive algorithm which uses an efficient data structure to obtain a global alignment. OpenCV (Drost et al., 2010) provides a surface registration algorithm which uses point pair features with hash table lookup and voting with pose clustering to obtain a global registration. The RANSAM method (Winkelbach et al., 2006) uses a point pair feature with hash tables to compute an initial alignment. We are motivated by the RANSAM approach but additionally use a surface curvature test to prune early the potential point pair hits in the hash table which improves robustness (see Section 3.1).

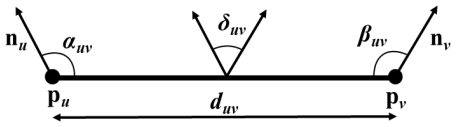

Figure 1: Illustration of 4D ($\alpha_{uv}, \beta_{uv}, \delta_{uv}, d_{uv},$) relation features for a point pair p_u and p_v.

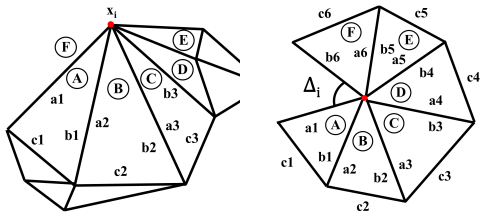

Figure 2: Efficient Gaussian curvature from discrete triangularization of the mesh. Δ_i is the angle deficit computed using the length a_i, b_i, c_i of the sides of the i^{th} triangle. (a) 3D view and (b) planar view.

3 MATHEMATICAL DETAIL

Let $\mathcal{P}_A = [p_1, ..., p_k]$ and $\mathcal{N}_A = [n_1, ..., n_k]$ be 3D points and corresponding surface normals of a surface A respectively. The combination of point with normal is referred as an *oriented point* (see 1). Let the set of oriented points $\mathcal{A}$ of surface A and oriented points $\mathcal{B}$ of surface B be

$$\begin{aligned} \mathcal{A} &:= \left\{ u = [p_u, n_u] \,|\, p_u \in \mathcal{P}_A \quad \text{and} \quad n_u \in \mathcal{N}_A \right\} \\ \mathcal{B} &:= \left\{ v = [p_v, n_v] \,|\, p_v \in \mathcal{P}_B \quad \text{and} \quad n_v \in \mathcal{N}_B \right\} \end{aligned} \tag{1}$$

Consider pairs of candidate matching points $a, c \in \mathcal{A}$ and $b, d \in \mathcal{B}$, two pre-defined frames can be used to determine a homogeneous 4×4 transformation $\mathbf{T} = [\mathbf{R}_{3\times3} \quad \mathbf{t_{3\times1}}; \quad 0_{1\times3} \quad \mathbf{1}]$ that optimally and robustly aligns the dipoles (a, c) and (b, d) such that

$$\mathbf{T} = F(a,c)^{-1}.F(b,d) \tag{2}$$

where the function $F(u, v)$ or F represents a coordinate system lying between oriented points u and v

$$F := \begin{bmatrix} \frac{p_{uv} \times n_{uv}}{\|p_{uv} \times n_{uv}\|} & p_{uv} & \frac{p_{uv} \times n_{uv} \times p_{uv}}{\|p_{uv} \times n_{uv} \times p_{uv}\|} & \frac{p_u + p_v}{2} \\ 0 & 0 & 0 & 1 \end{bmatrix} \tag{3}$$

where $p_{uv} = {}^{(p_v - p_u)}/_{\|p_v - p_u\|}$ and $n_{uv} = n_u + n_u$. Singular frames are avoided by ensuring the length of p_{uv} and n_{uv} is not zero.

3.1 GRANSAM

Gaussian curvature is an intrinsic surface property, i.e., isometrically invariant under rigid transformation (Besl and Jain, 1986). The standard Gaussian curvature computation (with derivatives) over the mesh requires computationally expensive per vertex local neighbourhood operations such as Eigen value decomposition of the covariance matrix (Besl and Jain, 1986; Rantoson et al., 2016). Instead, we use discrete triangularization of the surface to efficiently compute Gaussian curvature over the mesh (Besl and Jain, 1986). Consider a point x_i (*Red circle*) on the mesh which is a vertex for N different triangles as shown in the Figure 2. The Gaussian curvature for a point x_i can be computed as

$$K(x_i) = \frac{2\pi - \sum_{i=1}^{N} \Delta_i}{\sum_{i=1}^{N} \Lambda_i} \tag{4}$$

where $\Lambda_i = \sqrt{s(s-a_i)(s-b_i)(s-c_i)}$ is the area of triangle, with semiperimeter $s = {}^{a_i+b_i+c_i}/_2$, Δ_i is the angle deficit

$$\Delta_i = \arccos\left(\frac{a_i^2 + b_i^2 - c_i^2}{2a_i b_i}\right) \tag{5}$$

and a_i, b_i, c_i are the length of the sides of the i^{th} triangle. In practise, we use an approximated Gaussian curvature as

$$K(x_i) = 2\pi - \sum_{i=1}^{N} \Delta_i \tag{6}$$

Our GRANSAM uses the same 4D relation table as used in RANSAM (Winkelbach et al., 2006) consisting of the Euclidean distance d_{uv} between points, the angle of inclination α_{uv} and β_{uv} between the normals n_u and n_v, the line connecting p_u and p_v, and the rotation angle δ_{uv} between the normals around the connection line as shown in Figure 1. The rel(u,v) or rel is computed as

$$\text{rel} := \begin{bmatrix} d_{uv} \\ \cos\alpha_{uv} \\ \cos\beta_{uv} \\ \delta_{uv} \end{bmatrix} = \begin{bmatrix} \|p_v - p_u\| \\ n_u \cdot p_{uv} \\ n_v \cdot p_{uv} \\ \tan^{-1}\left(\frac{n_u \cdot (p_{uv} \times n_v)}{(n_u \times p_{uv}) \cdot (p_{uv} \times n_v)}\right) \end{bmatrix} \tag{7}$$

We also use the same match quality metric Ω as used by RANSAM (Winkelbach et al., 2006) to evaluate the transformation $\mathbf{T}$ computed using the pair of matches,

$$\Omega = \frac{\sum_{u,v=1}^{k} \begin{cases} 1 & \min \|\mathbf{T}p_u - p_v\| < \varepsilon \\ 0 & else \end{cases}}{k} + \frac{1.96}{2\sqrt{k}} \tag{8}$$

Algorithm 1: Our GRANSAM method.

Input:
Set of oriented points $\mathcal{A}$ of surface A and oriented points $\mathcal{B}$ of surface B.
Threshold ξ=0.1.
Output: Transformation matrix $\mathbf{T}$ which aligns $\mathcal{A}$ to $\mathcal{B}$.

1. Compute Gaussian curvature K for surface A and B using Equation 6.
2. Randomly choose oriented point pair $a, c \in \mathcal{A}$ and calculate rel(a,c) using Equation 7.
3. Insert it into the relation table for surface $\mathcal{A}$: such as $R_A[\text{rel}(a,c)] = (a,c)$.
4. Read the same position in the relation table for surface $\mathcal{B}$: $(b,d) = R_B[\text{rel}(a,c)]$.
5. If entry exists, verify if $|K(a) - K(b)| < \xi$ and $|K(c) - K(d)| < \xi$ then compute $\mathbf{T}$ for (a,b,c,d) using Equation 2 and 3, and estimate match quality Ω using Equation 8.
6. Randomly choose oriented point pair $b, d \in \mathcal{B}$ and calculate rel(b,d) using Equation 7.
7. Insert it into the relation table for surface $\mathcal{B}$: such as $R_B[\text{rel}(b,d)] = (b,d)$.
8. Read the same position in the relation table for surface $\mathcal{A}$: $(a,c) = R_A[\text{rel}(b,d)]$.
9. If entry exists, verify if $|K(a) - K(b)| < \xi$ and $|K(c) - K(d)| < \xi$ then compute $\mathbf{T}$ for (a,b,c,d) using Equation 2 and 3, and estimate match quality using Equation 8.
10. Repeat steps 2-9 until match quality is good enough or iteration limit is exceeds.

where k is the number of points, subscript $u = 1, ..., k$ and $v = 1, ..., k$. (see our Algorithm 1)

4 EXPERIMENTAL RESULTS

We have conducted a series of experiments to compare the performance of our GRANSAM method against state-of-the-art global registration methods RANSAM, FGR and MFR on two real world data sets, i.e., our 3D printed part dataset and the publicly available UWA benchmark dataset (Mian et al., 2006). Synthetic experiments have not been considered as 3D registration methods operating well on simulated dataset do not necessarily perform well on real world dataset. Our 3D printed part dataset is used to test the performance of 3D registration methods to align individual views of a single part to a reference multi-view model or CAD model. It contains partial views of challenging engineering parts with planar surfaces. The UWA dataset tests the ability to deal with multiple objects, clutter, occlusion

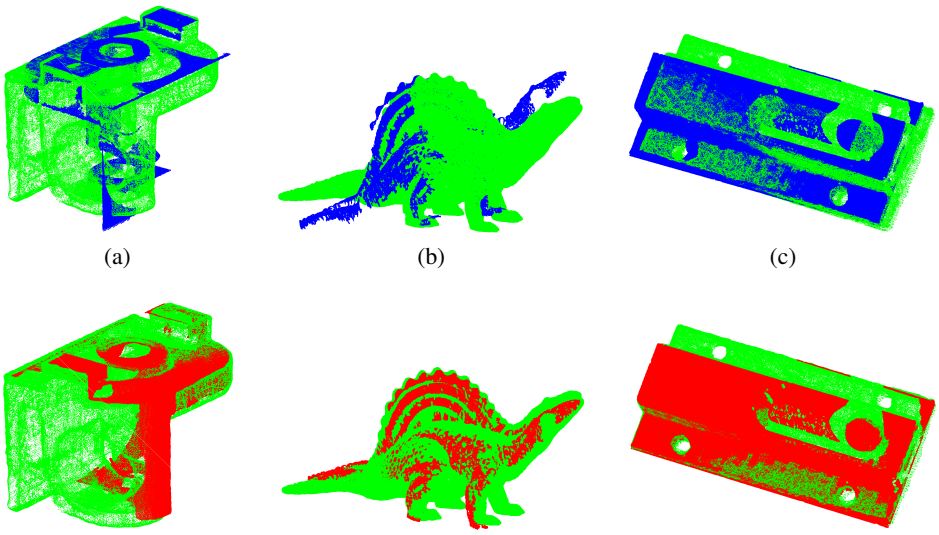

(a) (b) (c)

(d) (e) (f)

Figure 3: RANSAM (*Blue points*) versus GRANSAM (*Red points*) registration on model (*Green points*). (a, b, c) v.s (d, e, f) for Extruder, Dinosaur and Slide lock respectively. Note misalignment in *top* versus *bottom* row (zoom in PDF to see detail).

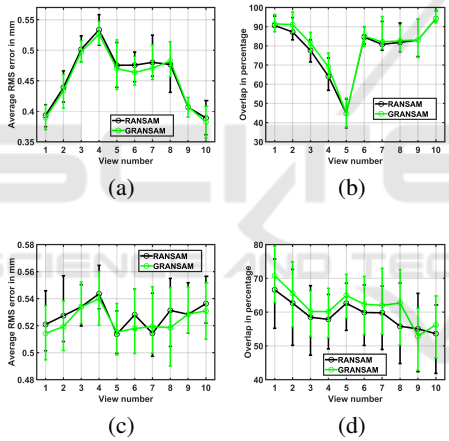

(a) (b)

(c) (d)

Figure 4: RANSAM (*Black line*) versus GRANSAM (*Green line*) 3D registration on Extruder (*top row*) and Bunny (*bottom row*). (a)-(c) RMS point-to-point error in mm and (b)-(d) corresponding overlap in percentage.

and low overlap. Our GRANSAM method which outperforms FGR and MFR can also be considered to surpass the performance of six other global registration methods (termed as GoICP, GoICP-Trim, Super4PCS, OpenCV PCL and CZK).

4.1 3D Printed Part Dataset

This dataset consists of six models (Extruder, Dinosaur, Slide lock, Bunny, Focus housing and Camera mount) which are captured from 10 different views, i.e., a total of 60 scans for testing GRANSAM versus RANSAM registration. The Figure 3 shows the accurate GRANSAM (*Red points*) registration versus misaligned RANSAM (*Blue points*) registration on model (*Green points*). In our experiments, GRANSAM's Gaussian curvature pruning consistently obtained better registration than RANSAM.

We applied the GRANSAM and RANSAM method 100 times on the 3D printed part dataset to compute the average RMS error, overlap percentage, and computational time score. We use a threshold of 1 mm to compute the RMS error and overlap percentage. The Figure 4 shows the reduced average RMS and increased overlap in percentage of the GRANSAM versus RANSAM along with 25^{th} and 75^{th} percentiles of the population (which are shown as vertical bars) for each view of the Extruder and Bunny. GRANSAM's considerable improvement over RANSAM can be seen in certain views, for example, view 2, 3, 4 of the Extruder has reduced RMS error with up to 4.5% increase in overlap and view 1, 2, 8 of the Bunny has reduced RMS error with up to 12.5% increase in overlap. In our experiments, the reduction in RMS error and improvement in overlap percentage was observed in many views of the 3D printed part dataset. Note that as expected GRANSAM performance was better for objects with rough surface or crest and trough and was not improved for objects with planar surface. However, there are numerous real world shapes which have sufficient surface curvature where GRANSAM's Gaussian curvature based pruning will benefit any registration scheme.

In Table 1, we summarize the average RMS error in mm and overlap in percentage across all views

Table 1: Average across all views of the 3D printed part dataset: (1) Extruder, (2) Bunny, (3) Camera mount, (4) Dinosaur, (5) Focus housing, (6) Slide lock. Bold shows winner per category.

	RMS error in mm					
	1	**2**	**3**	**4**	**5**	**6**
RANSAM	0.46	0.42	0.21	0.53	0.26	0.37
GRANSAM	**0.45**	**0.41**	**0.21**	**0.52**	**0.25**	**0.36**
	Overlap in percentage					
	1	**2**	**3**	**4**	**5**	**6**
RANSAM	78.8	69.5	96.1	59.2	96.2	82.9
GRANSAM	**80.5**	**69.6**	**96.3**	**61.8**	**96.5**	**83.1**

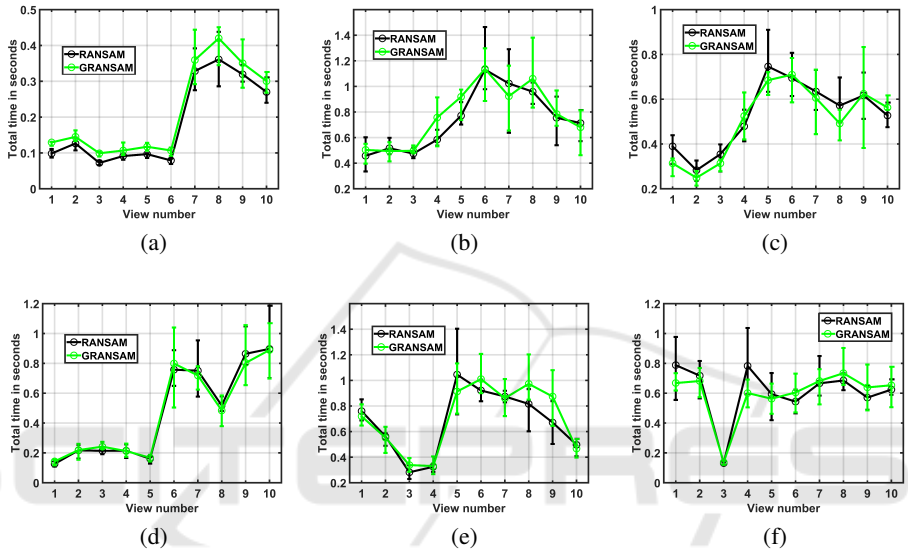

Figure 5: Comparison of the computational time in seconds for 3D registration obtained using RANSAM (*Black line*) and GRANSAM (*Green line*). (a) Extruder, (b) Bunny, (c) Camera mount, (d) Dinosaur, (e) Focus housing and (f) Slide Lock.

of the 3D printed part dataset using RANSAM and GRANSAM. The Figure 3, 4 and Table 1 show that our GRANSAM obtains more consistent registration than RANSAM.

Figure 5 shows that GRANSAM (*Green line*) has similar computational time as RANSAM (*Black line*) on the 3D printed dataset for a maximum of 5000 iterations per run. GRANSAM introduces minimal computational cost of up to 0.1 seconds (the cost of pre-computing the Gaussian curvature is very small, i.e., 1-10 milliseconds).

4.2 UWA Benchmark Dataset

This dataset consists of four models (Cheff, Chicken, Parasaurolophus, T-rex) with 50 scenes of multiple objects, i.e., all four objects are present in most of the scenes. Similar to (Zhou et al., 2016), a total of 188 model and scene pairs for testing registration. It is a challenging data set due to clutter, occlusion and low overlap between model and scene.

The Figure 6 shows the GRANSAM (*Red points*) registration versus misaligned RANSAM (*Blue points*) on model (*Green points*). It can be seen in Figure 6a-6b versus 6d-6e that RANSAM fails while GRANSAM correctly aligns the scene to the model.

In Figure 7, we summarize the average RMS error and overlap percentage across the 188 pairwise registration of the UWA dataset using FGR, MFR, RANSAM and GRANSAM method. It can be seen from Figure 7a that on average our GRANSAM method obtains a lower RMS error than FGR, MFR and RANSAM methods while maintaining good overlap percentage as shown in Figure 7b.

Table 2 summarizes the percentage reduction in *RMS* error using GRANSAM versus other methods on UWA dataset. Note that on average GRANSAM has a 37.73%, 37.03%, 7.84% reduction in RMS error versus FGR, MFR and RANSAM method respectively. Hence, GRANSAM is able to deal with low overlap, multiple objects and high occlusion UWA da-

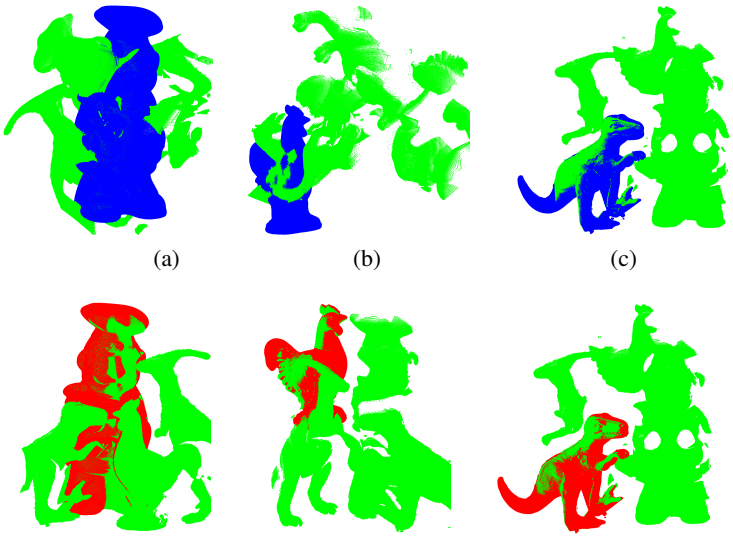

Figure 6: RANSAM (*Blue points*) versus GRANSAM (*Red points*) registration on model (*Green points*). Cheff, Chicken and T-rex left-to-right. Note misalignment in *top* versus *bottom* row (zoom in PDF to see detail).

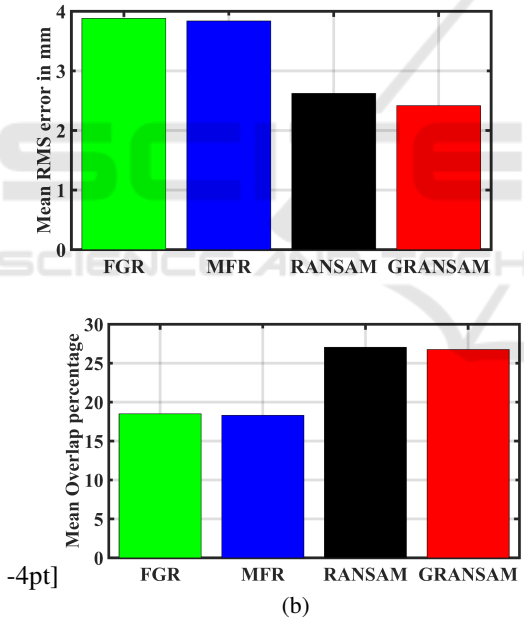

-4pt]

(b)

Figure 7: GRANSAM versus FGR, MFR, and RANSAM 3D registration on UWA dataset. (a) Mean RMS error and (b) mean overlap percentage.

taset and also surpasses the performance of six global registration methods (termed as GoICP, GoICP-Trim, Super4PCS, OpenCV PCL and CZK).

4.3 Computational Speed

GRANSAM has a low complexity of O(k) (Winkelbach et al., 2006). The computational time was measured in the Microsoft Visual Studio 2015 on a HP Z mobile workstation with an Intel i7 2.66 GHz processor with 16 GB RAM. GRANSAM and RANSAM both take in total about 3-6 seconds to compute the 3D registration between a scene and model. In contrast, the descriptor based FGR and MFR methods take in total about 30 seconds to a few minutes to compute the 3D registration depending on the number of points in the scene and model.

5 CONCLUSION

We have presented a discrete Gaussian curvature criterion based RANdom SAmple Matching (RANSAM) method to remove false matches to improve the accuracy of 3D registration while maintaining efficiency. The main novelty of our work is the inclusion of Gaussian curvature check to prune out mismatched point correspondences during shape alignment within the RANSAM framework. We avoid geometric features requiring computationally expensive accumulation or differentiation of local information and show that a simple and efficient discrete Gaussian curvature feature provides a powerful and easy to integrate descriptor to improve any 3D registration approach. The results on a number of shape alignment benchmark showed the considerable improvement in 3D registration by using the Gaussian curvature criterion.

Table 2: Percentage reduction in *RMS* error of GRANSAM versus other methods on UWA dataset.

	FGR	MFR	RANSAM
GRANSAM	37.73	37.03	7.84

REFERENCES

Besl, P. J. and Jain, R. C. (1986). Invariant surface characteristics for 3d object recognition in range images. *Computer Vision, Graphics, and Image Processing*, 33:33–80.

Choi, S., Zhou, Q.-Y., and Koltun, V. (2015). Robust reconstruction of indoor scenes. In *CVPR*, pages 5556–5565.

Drost, B., Ulrich, M., Navab, N., and Ilic, S. (2010). Model globally, match locally: Efficient and robust 3d object recognition. In *IEEE Conference on Computer Vision and Pattern Recognition*, pages 998–1005.

Faisal Azhar, S. P. and Adams, G. (2019). Modified m-estimation for fast global registration of 3d point clouds. In *Electronic Imaging*.

Fischler, M. A. and Bolles, R. (1981). Random sample consensus: A paradigm for model fitting with applications to image analysis and automated cartography. *ACM Commun.*, 24(6):381–395.

Gelfand, N., Mitra, N. J., Guibas, L. J., and Pottmann, H. (2005). Robust global registration. In *Proceedings of the Third Eurographics Symposium on Geometry Processing*. Eurographics Association.

Holz, D., Ichim, A. E., Tombari, F., Rusu, R. B., and Behnke, S. (2015). Registration with the point cloud library: A modular framework for aligning in 3-d. *IEEE Robotics Automation Magazine*, 22(4):110–124.

Mellado, N., Aiger, D., and Mitra, N. J. (2014). Super 4pcs fast global pointcloud registration via smart indexing. *Comput. Graph. Forum*, 33:205–215.

Mian, A. S., Bennamoun, M., and Owens, R. (2006). Three-dimensional model-based object recognition and segmentation in cluttered scenes. *IEEE Trans. Pattern Anal. Mach. Intell.*, 28:1584–1601.

Rantoson, R., Nouira, H., Anwer, N., and Mehdi-Souzani, C. (2016). Improved curvature-based registration methods for high-precision dimensional metrology. *Precision Engineering*, 46:232 – 242.

Rusu, R. B., Blodow, N., and Beetz, M. (2009). Fast point feature histograms (fpfh) for 3d registration. In *Proceedings of IEEE International Conference on Robotics and Automation*, pages 1848–1853.

Rusu, R. B., Blodow, N., Marton, Z. C., and Beetz, M. (2008). Aligning point cloud views using persistent feature histograms. In *Proceedings of the 21st IEEE/RSJ International Conference on Intelligent Robots and Systems*.

Tombari, F., Salti, S., and Di Stefano, L. (2010). Unique signatures of histograms for local surface description. In *Proceedings of the 11th European Conference on Computer Vision Conference on Computer Vision: Part III*, ECCV'10, pages 356–369.

Winkelbach, S., Molkenstruck, S., and Wahl, F. M. (2006). Low-cost laser range scanner and fast surface registration approach. In *Pattern Recognition*, pages 718–728.

Zhou, Q.-Y., Park, J., and Koltun, V. (2016). Fast global registration. In *ECCV*, pages 766–782.